

Function Field Analysis for the Visualization of Flow Similarity in Time-Varying Vector Fields

Harald Obermaier and Kenneth I. Joy

Institute for Data Analysis and Visualization, University of California, Davis, USA

Abstract. Modern time-varying flow visualization techniques that rely on advection are able to convey fluid transport, but cannot provide an accurate insight into local flow behavior over time or locally corresponding patterns in unsteady vector fields. We overcome these limitations of purely Lagrangian approaches by generalizing the concept of function fields to time-varying flows. This representation of unsteady vector-fields as stationary function fields, where every position in space is a vector-valued function supports the application of novel analysis techniques based on function correlation, and allows to answer data analysis questions that remain unanswered with classic time-varying vector field analysis techniques. Our results demonstrate how analysis of time-varying flow fields can benefit from a conversion into function field representations and show the robustness of our presented clustering techniques.

1 Introduction

In areas such as meteorology or aerodynamics complex flow fields are being produced whose analysis and interpretation requires the development of suitable visualization techniques. There are flow analysis problems, e.g., in meteorology, that are, unlike many modern flow analysis approaches, not only concerned with the transport behavior of flow, but with the detection, and analysis of (repeating) local flow behavior. Previously, this important task has rarely played a role during the design process of unsteady flow visualization techniques.

We develop new methods that aim at supporting this task by visualizing flow similarity and allowing analysis and discovery of similar or relevant local behaviors in the flow field. For this matter, we interpret unsteady flow fields as stationary function fields. With this notion we are able to apply function processing and cross-correlation concepts and develop meaningful flow similarity metrics. These novel metrics are used for automatic flow domain clustering and manual flow behavior querying and prove to be valuable in answering relevant flow analysis questions that are hard to answer with existing techniques. Our visualization solution reduces the visual complexity of multi-temporal flow visualization that often suffers from the presence of features with a spatio-temporal character, such as path-lines. For the first time, it is now possible to identify regions that yield similar flow behavior over time, a notion that is of central importance in location based flow analysis such as in meteorology or geometry optimization in aerodynamics and industrial mixing. Furthermore, our novel techniques support interactive querying in vector-valued function fields.

Section 2 summarizes related work and provides a motivation. Section 3 introduces function fields, before novel flow similarity metrics are presented in Section 4. Visualization and analysis techniques are detailed in Section 5, whereas concrete results are presented in Section 6. Section 7 concludes this work.

2 Motivation and Related Work

Most modern unsteady flow analysis techniques focus on the analysis of material transport and the extraction of flow trajectories [1, 2], mimicking physical experiments such as dye advection in a Lagrangian setting. Even in combination with querying [3–6], these analysis techniques neglect a large field of application areas, where recurring patterns [7–9] and local flow behavior is of central importance. In such contexts, a Eulerian perspective of the flow field is more suitable for effective visual analysis.

In meteorology, for example, the behavior of wind directions in town X in a given month may be compared to wind behavior at a different location during the same time period. Alternatively, wind behavior may be studied at the same location for different seasons. In combination, this requires a multi-temporal, local analysis of flow. Physically, such Eulerian flow measurements may be obtained e.g., by means of Doppler Velocimetry [10]. Here, no longer is fluid transport the focus of interest, but characteristics of local flow behavior over time and space.

Changing the representation of an unsteady vector field into a different form (cf. FTLE [11] or scalar function fields [12]) has long known to make certain analysis and visualization tasks feasible or computationally more straight-forward. We therefore choose to represent unsteady flow as vector-valued function fields. This localized representation supports the use of flow pattern recognition, tracking, and querying of similar local flow behaviors. These techniques are related to research [13–15, 5] on time-series, where 2D graphs [16] still dominate the field. For the first time, the presented techniques allow automatic time-varying flow similarity analysis, straight-forward identification of 'dead' mixing regions and interactive behavior querying. Thus, we regard function field representations as suitable solutions to local flow analysis problems. The workflow structure of the remainder of this paper is illustrated in Figure 1.

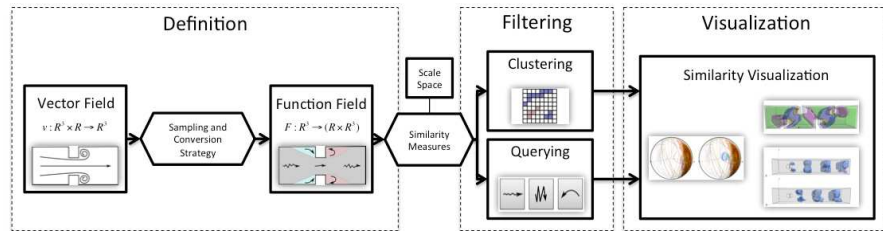


Fig. 1. Workflow of flow similarity evaluation. Definition of similarity measures supports clustering and querying of similar flow behavior in a function field.

3 Function Fields

3.1 Definitions and Concepts

A time-varying 3D flow field $v : \mathbb{R}^3 \times \mathbb{R} \rightarrow \mathbb{R}^3$ is a continuous representation of velocity vectors at positions $x \in \mathbb{R}^3$ and time $t \in \mathbb{R}$. An equivalent notion of such a flow field can be obtained by modifying the role of an independent variable:

$$F : \mathbb{R}^3 \rightarrow (\mathbb{R} \rightarrow \mathbb{R}^3) \quad (1)$$

$$F(x) = v(x, \cdot) \quad (2)$$

F contains a vector-valued function at every position in space and is therefore called a *function field*. An individual vector-valued function at position $x \in \mathbb{R}^3$ in F is denoted by f_x and called a *local flow pattern* in the following. A *normalized* flow pattern corresponds to a normalized v with unit vectors. Note that there may be equivalent flow patterns at different positions in the flow field, for which reason the position index may be dropped. This representation is comparable to feature-space representations used in visualization as it represents a set of (independent) functions. For scalars, such a notation was used by Anderson et al. [12]. A *flow motif* is obtained by restricting the parameter space of a flow pattern to an interval $[t_0, t_1] \subset \mathbb{R}$. We denote such a flow motif as $(f_x, [t_0, t_1])$.

3.2 Function Field Creation

The conversion of an unsteady flow field into its numerical representation as a function field requires finding an appropriate sampling strategy for the placement of local flow functions. We propose the use of three alternative sampling strategies. The first and most simple strategy uses a regular grid [17] to position local flow patterns. This is fast to compute and facilitates flexible user control along with level-of-detail sampling. Since the visual output of the techniques presented in this paper does not directly depend on the density and uniformity of the chosen sampling, we can make use of further techniques. The second strategy places a flow function at every node of the original computational grid of the flow field. This technique has a more optimal sampling resolution, but is only applicable to fields that maintain a static mesh. The third approach adaptively samples the flow field. In this approach we construct a octree representation of the flow field whose cells are subdivided if they span a region with a large variance in velocity direction at any point in time (see Figure 2a). In all cases, a single local flow pattern f_x represents the flow direction of a constrained region $C \subset \mathbb{R}^3$ (cell) of the flow field. Numerically, a flow pattern f_x is stored as a series of average vector values $[v(x, t_0), \dots, v(x, t_n)]$ together with standard deviations of velocity $[SD(C, t_0), \dots, SD(C, t_n)]$ computed from discrete velocity histograms per cell C and time step. Note that standard deviations for strategies whose grid cells correspond to less than a cell in the original resolution evaluate to zero. In the course of this paper we normalize all flow patterns to $f_x(\cdot)/\|f_x(\cdot)\|$. Flow patterns with a standard deviation magnitude above 1 are considered non-representative and dissimilar to all other patterns.

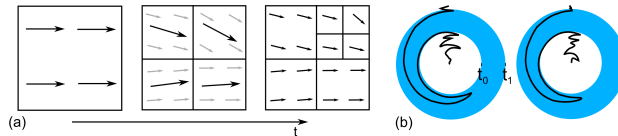


Fig. 2. (a) Cell subdivision in octree sampling is based on time-varying velocity deviation. If velocities within a cell are too dissimilar in a time step, it is subdivided. (b) Illustration of 2D flow radar glyphs as introduced in [17]. Our motif similarity extraction supports the detection of similar flow behavior as highlighted in blue.

4 Flow Similarity

Consisting of a set of independent, local flow patterns, the function field representation is a suitable tool for local, domain centered flow analysis. Through pattern clustering, the identification of dead regions, recurring flow patterns, and distinct flow behaviors may be achieved. Metrics for the efficient, manual and automatic local flow pattern similarity evaluation are presented in the following.

4.1 Visual Similarity

With a direct function visualization technique, similarity evaluation in a function field may be performed visually. An example of such a technique are flow radar glyphs that map flow directions to curves on a radial glyph [17]. While the proposed glyphs (Figure 2b) are a step towards analysis of unsteady flow, there are limits w.r.t. accurate similarity evaluation and expressiveness as the number of time-steps is increased. In this work we devise methods to effectively display and analyze flow behavior similarity in unsteady 3D flow.

4.2 Similarity Metrics

The key to efficient clustering and similarity analysis in function space is the definition of mathematical distance measures d for any two flow motifs f and g that allow efficient and meaningful comparison of flow patterns. In the context of this work we identify the following key characteristics of flow distance measures:

- **Efficiency:** d should be fast to compute to facilitate interactive querying.
- **Robustness:** Influence of small scale noise from the simulation on the value of d is to be reduced.
- **Flexibility:** d should be invariant w.r.t. selected linear transformations such as rotation or scaling of patterns.

The flexibility criterion exists to support not only analysis of direct similarity between flow functions (i.e., $d(f, g) = 0$ iff $f = g$), but also facilitate similarity comparison with respect to abstract flow behaviors (i.e., oscillation along an arbitrary direction, $d(f, g) = 0$, iff $f = Rg$, with linear transformation R). Thus, similarity of local flow patterns is defined on multiple levels of abstraction. In the following we provide details about similarity measures on two levels of abstraction. In the remainder of this work we assume normalized flow motifs.

Relative Similarity A low-level similarity comparison only requires direct comparison of functions. Ideally, behavioral similarity that includes linear transformations is computed by maximizing similarity with respect to a linear transformation matrix R . Function similarity or (cross-)correlation is commonly based on application of the inner product over the range of two functions. We therefore adopt a modified version of the discrete maximum norm

$$d(f, g) = \min_R(\max_t(1 - \langle f(t), Rg(t) \rangle \cdot s(t))), \quad (3)$$

where Euclidean distances in standard deviations are used to modify the value of the inner product in the form of $s(t) = 1 - |\text{atan}(\|SD_f(t) - R \cdot SD_g(t)\| \frac{2}{\pi})|$. Numerically the arctangent is approximated by a second order polynomial. For computational efficiency, we approximate this similarity by first computing average flow direction of f and g : \bar{f} and \bar{g} , which are used to align f and g , such that $\bar{f} = \bar{g}$. Finally, we rotate g around \bar{g} until $d(f, g)$ is minimal. This rotation is performed in 20 degree angles and uses angle bisection to iterate to maxima. Note that simply choosing $R = I$ violates the flexibility criterion, but still allows for simple function comparison. This distance measure identifies flow behaviors that are identical under rotational transformation and returns overall maximal angular deviation between velocities present in flow patterns.

Behavioral Similarity A more abstract measure compares similarity of abstract flow behaviors. For this matter, a vector-valued function has to be converted into a behavior-sequence description. We exploit the fact that a range of typical flow behaviors can be described mathematically and be used to classify flow motifs. We identify these typical flow behaviors B (see Figure 2b for backflow) as boolean predicates on flow motifs $(f, [t_0, t_n]) = (f(t_0), \dots, f(t_n))$:

- **P(Constant) = true** iff time-variation of flow direction is minimal.
 $f(t) \cdot \bar{f} < \epsilon$ for all $t \in [t_0, t_n]$, \bar{f} average flow direction of the motif.
- **P(Oscillation) = true** iff velocity directions oscillate along a direction.
 $|\angle(f(t_i) - f(t_{i-1}), f(t_{i+1}) - f(t_i))| \ll \frac{\pi}{2}$ for subsequent i .
- **P(Backflow) = true** iff flow direction is inverted.
 $f(t) \cdot \bar{f} \ll 0$ for at least one $t \in [t_0, t_n]$
- **P(Rotation) = true** iff flow directions rotate around a center direction c .
 $\angle(f(t_{i-1}) - c, f(t_i) - c) \cdot \angle(f(t_i) - c, f(t_{i+1}) - c) > 0$
 $\sum \angle(f(t_i) - c, f(t_{i+1}) - c) > 2\pi$, $|\angle(f(t_i) - f(t_{i-1}), f(t_{i+1}) - f(t_i))| < \epsilon$.
- **P(Swirling) = true** iff flow performs planar rotation.
 Same as rotation, but $\bar{f} \approx 0$

Note that behaviors based on velocity magnitude, such as pulsation are excluded from this paper and are subject to future research. Every one of these behaviors B may hold for a given flow motif. Thus, a local flow pattern shows a selected behavior B for a length $t_1 - t_0$ if it contains a flow motif $(f, [t_0, t_1])$ with $P(B) = \text{true}$. This allows for behavior querying and distance computation. A flow pattern is converted into a sequence of flow behaviors by performing a

sliding-window search with varying window length according to user specified minimal and maximal window lengths. This creates flow motifs for the evaluation of behavior predicates. At every point in time, the B that holds for a maximal window length is selected. For equal lengths, priorities are Constant < Oscillation < Backflow < Rotation < Swirling. If no pattern matches, behavior is assumed to be chaotic. Two flow patterns are considered similar if they represent the same sequence of flow behaviors. The distance function then evaluates to the Euclidean distance between the behavior-length vectors of the two functions.

4.3 Improvements

In combination, the presented similarity measures satisfy all key requirements listed in the last section with exception of robustness with respect to noise in the spatial and time dimension. We implement a scale space representation along with a time-shift similarity measure to allow for robust similarity evaluation.

The representation of flow patterns as vector-valued functions allows the application of concepts from scale space theory. Thus, we represent individual flow patterns as one parameter family of low-pass filtered [13] curves. Consequently, we do not use f and g in (3), but the resulting curves after Gaussian filtering with different kernel widths. This reduces the impact of small scale variations in matching and allows robust scale-based matching with a user-specified scale.

The time-varying nature of our problem can cause different locations in the flow field to show very similar flow behavior at slightly different times. Thus, a rigid comparison based on flow pattern entries at corresponding times (static inner-product in (3)) is inferior to time shift matching methods. Consequently, we implement the *Dynamic Time Warping* (DTW) [18] method to provide a time-shift tolerant similarity measure between flow patterns.

5 Function Field Analysis and Visualization

Clustering of function fields based on the presented distance measures can help identify similar and relevant behaviors automatically. However, in flow analysis, interactive exploration of flow properties is often superior to automatic feature detection, making the definition of suitable operators necessary. Thus, we allow the application of feature space querying techniques [19, 6] to function fields. We make use of semantically linked visualizations of the function field along with its domain geometry and a visualization of function space for efficient querying and cluster representation as described in the following.

Function Space Visualization We use a spherical representation for the visualization of function space that maps flow motifs to radial curves in a sphere [20, 15]. Goal of this visualization is to plot all or a selection of normalized patterns in a common space in a manner that allows a concise overview of the behavior of the set of patterns with respect to time and orientation. Additionally, we facilitate brushing operations such as pattern selection and region of interest selection

on the surface of the sphere. The user is enabled to draw on the sphere to mark and filter individual behaviors. The visualization of this potentially vast amount of functions, as well as temporal components require special attention.

As a first step, we create curve geometry on the GPU to allow interactive framerates in the presence of a large number of curves. The resulting curve geometry, projected polygon strips, are color coded by t , and blended together in order to emphasize behaviors that are present in multiple flow patterns. While this gives a good impression of the distribution of orientations throughout the parameter space of the flow field, it still lacks an expressive notion of time, even when the rendered curves are color-coded. Radially scaling these functions according to time allows efficient perception of temporal characteristics, similar to generalized flow radar glyphs. For joint behavior analysis, we offer the option to rotate all flow patterns such that all average flow pattern directions line up, giving a better insight into backflow, rotation and overall constant behavior. We optionally visualize clusters of flow motifs or subsets of function space as separate spherical plots by filtering out flow patterns that do not belong to a cluster.

Function Field Visualization Clustering, similarity evaluation, and querying results in the selection of (possibly disconnected or overlapping) flow motifs, i.e., spatio-temporal selections in the function field domain. Visualization of these function sets requires the simultaneous display of individual and compound function properties. On an individual function level, we draw a single generalized flow radar glyph at the position of flow patterns. If only a specific time range of the function (i.e. a flow motif) is selected, the corresponding glyph is faded out if the currently displayed time step is outside of the range of the motif.

To highlight the shape and geometry of the current position of a cluster of motifs, we extract a metaball based [21] isovolume for each cluster, thus giving an insight into positions of selected function sets. Metaballs are scaled according to the selected function cell size. We provide the user with a region-of-interest selection tool that allows the selection of a set of local flow patterns in space followed by a specification of the relevant time interval. This effectively selects flow motifs in the function field. Furthermore, the user can query for behaviors B in the flow field by composing a sequence of behaviors.

6 Results

We demonstrate the efficiency and applicability of function field analysis with the help of selected data sets that were generated by flow simulations and converted into function field representation by uniform sampling with up to 10000 flow patterns. Functions are represented at 10 scales, around 30 time steps were processed per simulation.

6.1 Performance

During pre-processing, the field is evaluated and converted into function field representation. The speed of these operations is directly dependent on the field evaluation method, number of time-steps, and sampling strategy/density. These computations took less than a minute for all presented data sets on a 64 bit Intel Corei7 at 2.2 Ghz with 8 GB of memory.

In Figure 3b we present average computation times for automatic clustering of the function field for different numbers of clustered flow observers and two different clustering techniques. The *distance* times denote time spent to compute a full similarity matrix for all patterns. Note that distance computation, as is used during interactive querying as well, is fast even for large numbers of flow patterns, which clustering techniques with quadratic or higher complexity become unfeasible for very large numbers of patterns. In practice this can be avoided by restricting function field analysis locally.

6.2 Clustering and Querying

We perform automatic clustering of flow regions by k-means or QT-clustering [22] with (3). QT-clustering, a method that creates a clustering given a specified maximal intra-cluster distance, of an extraction column data set reveals large sets of similar flow behavior and produces a decomposition into regions with persistent flow behavior. Sphere-plot visualizations of the user selection and the 11 largest clusters are shown in Figure 3a. Clustering reveals regions with distinct flow behaviors as indicated by a range of different cluster variances and oscillation patterns. This shows how the local effects of boundary properties like corners or flow obstacles onto the flow field can efficiently be detected, visualized, and analyzed as indicated by pockets of turbulent flow behind flow obstacles. The mixing column example hints at possible applications in medical areas, where the effect of blood-vessel anomalies on local blood flow have to be studied. As demonstrated in this figure, function field analysis can answer the abstract question "*Where in this data set do similar 'flow events' happen?*" in time-varying flow fields. Furthermore, flow pattern clustering is able to reveal symmetries in the flow field. The shown flow-fields are virtually symmetric along their x-axis (z-axis), as shown by extracted pattern outlines. This represents a novel way of analyzing time-varying flow symmetries, which could not be captured by previous visualization methods. Automatic clustering of flow fields in a spatio-temporal setting has potential application areas in flow field compression or acceleration of trajectory computation. In our given example, we can clearly distinguish different constant and unsteady flow behaviors, i.e., regions where time plays a minor vs. a major role.

Function space visualization and brushing is useful, if overall flow behaviors in the data set are to be visualized or analyzed. We have implemented proof-of-concept techniques for the described brushing operations in function-space. We use interactive sphere brushing for pattern selection on the sphere plot, performing brushing in time-varying space of flow patterns and orientations. We

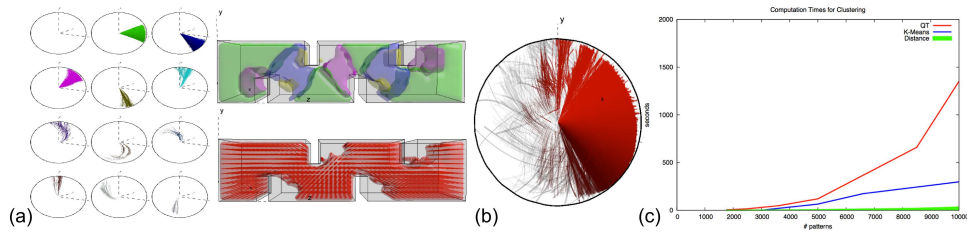


Fig. 3. (a) Result of QT clustering on an extraction column data set. Visualization shows user selection (top left) and the 11 largest clusters produced by QT clustering. The four largest clusters are rendered in the data set (top). The different flow behaviors in these regions is clearly depicted in the spherical plots. The 3D visualization facilitates analysis of similar, low, and high turbulence regions, supporting analysis of mixing properties. A cluster obtained by querying for constant flow is shown at the bottom along with vector splats indicating flow direction. (b) Constant flow selection shown in function space. Comparatively low variance in the green, blue and purple regions indicate large regions with linear, homogeneous flow behavior. (c) Computation times for clustering.

employ a simple combination of ray-sphere intersection and stencil-buffering to allow selection of regions on the sphere. Selected flow patterns are found by collecting vertices of the projected flow pattern representation on the sphere that lie within the selected region-of-interest. Such brushing queries can reach from simply selecting regions that have backflow behavior at a certain point in time over to querying flow patterns that have comparable turbulence or oscillation properties. Figure 4 shows the effect of function rotation and possible manual selections. In the shown cross-flow data-set, distinct rotating backflow behavior can be identified as the flow passes sharp corners. Virtually all other flow regions are covered by constant flow, as indicated by generalized flow radar glyph visualization and metaball-based selection outlining. The given function space visualization indicates locations, time, and extend of backflow in different regions of the data set and enable direct filtering or highlighting of such flow patterns. Direct manual function space operations together with metaball visualization are able to discover small scale boundary effects on the flow field that are hidden with glyph-based rendering techniques.

A jet stream data set is displayed in Figure 5. Function space display in such a turbulent data set becomes challenging if no flow patterns are pre-filtered by automatic clustering. Automatic and manual clustering highlights relevant flow behaviors and emphasizes a point-symmetry present throughout the complete evolution of the data set.

We recorded motifs by region-of-interest selection in the function field domain close to vortex cores in a simulated Kármán vortex street. Similarity evaluation highlights flow motif sets in other regions in space and time of the data set that behave similarly to the recorded motif set, see Figure 6. The results of such motif recording are promising for two reasons: They can be applied to detect and track

flow anomalies in flow fields and to uncover error sources such as faults in the simulation code or mesh.

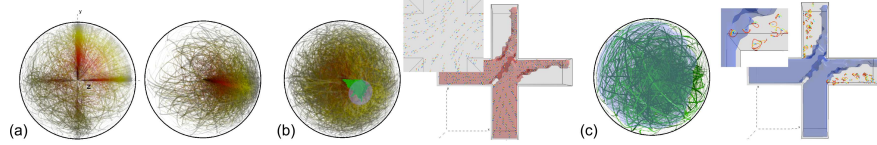


Fig. 4. (a) Feature space visualization without average direction alignment and with average direction alignment. Note the four distinct flow directions in the non-rotated rendering. (b) Manual selection of flow patterns with constant flow behavior. Metaball outlining gives a look at set outlines, revealing a small region around the bottom left inner corner, where non-linear flow occurs. (c) Manual selection of pattern with backflow behavior. A close-up illustrates, how different flow patterns as glyphs may appear despite having similar flow behaviors. This illustrates, why pure visual comparison of flow glyphs is not sufficient for accurate similarity analysis.

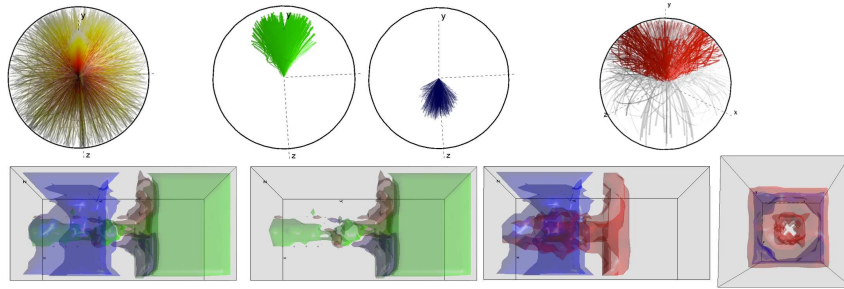


Fig. 5. Analysis of a short sequence of a jet flow data set reveals multiple orthogonal flow behaviors. Automatic clustering produces homogeneous constant backflow and forward (at the front and center) flow clusters and emphasizes point-symmetry of the data set. Note that function space display alone without cluster information is not expressive for this data set. Manual querying in function space allows the extraction of flow details, such as the main jet core shown from the side and front.

7 Conclusions and Future Work

In this work we have presented techniques to create and utilize a function field definition for unsteady flow fields. This conversion allowed the definition of effective function space similarity measures that support novel unsteady vector-field analysis and visualization techniques based on flow behavior similarity and

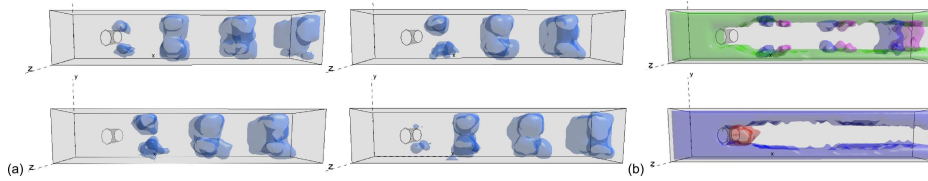


Fig. 6. (a) Flow pattern recording in a Kármán vortex street. Distinct flow behaviors are reliably tracked over time. An interesting property made evident by this visualization is the fact that these features are born on both sides of the obstacle and merge after passing the region with prominent backflow behavior. (b) Results from automatic clustering (top) reveal the spatial frequency of recurring flow behavior. Constant and backflow behavior querying (bottom) show regions unaffected by turbulent vortex core paths.

clustering. Function field representations and processing techniques allow unsteady flow field analysis that is not possible with transport based Lagrangian approaches. A set of presented querying and visualization techniques facilitates interactive function field analysis in a wide number of potential application areas. A drawback of the presented methods is their limitation to normalized flow patterns, while this can be compensated by taking spatial variation of velocity vectors into account, it cannot model behaviors based on velocity magnitude. Future work is focused on the creation and evaluation of further interaction techniques, such as interactive flow observer placement and the evaluation of function field techniques in concrete application areas.

Acknowledgements

The authors wish to thank the members of the Institute for Data Analysis and Visualization (IDAV) for valuable discussions and support.

References

1. Weiskopf, D., Erlebacher, G.: Flow visualization overview. In: Handbook of Visualization, Elsevier, Amsterdam (2005) 261–278
2. McLoughlin, T., Laramee, R.S., Peikert, R., Post, F.H., Chen, M.: Over two decades of integration-based geometric flow visualization. *Comp. Graph. Forum* **29** (2010) 1807–1829
3. Shi, K., Theisel, H., Hauser, H., Weinkauff, T., Matkovic, K., Hege, H.C., Seidel, H.P.: Path line attributes - an information visualization approach to analyzing the dynamic behavior of 3d time-dependent flow fields. In: *Topology-Based Methods in Visualization II, Mathematics and Visualization*. Springer (2009) 75–88
4. Xu, L., Shen, H.W.: Flow web: a graph based user interface for 3d flow field exploration. *Visualization and Data Analysis 2010* **7530** (2010) 75300F
5. Wei, J., Wang, C., Yu, H., Ma, K.: A sketch-based interface for classifying and visualizing vector fields. In: *In Proc. of PacificVis'10*. (2010) 129–136

6. Lez, A., Zajic, A., Matkovic, K., Pobitzer, A., Mayer, M., Hauser, H.: Interactive exploration and analysis of pathlines in flow data. In: Proc. Int. Conf. in Central Europe on Comp. Grap., Vis. and Comp. Vision (WSCG 2011). (2011) 17–24
7. Garcke, H., Preußer, T., Rumpf, M., Telea, A., Weikard, U., van Wijk, J.: A continuous clustering method for vector fields. In: Proc. of the Conf. on Visualization '00, Los Alamitos, CA, USA, IEEE Computer Society Press (2000) 351–358
8. Schlemmer, M., Heringer, M., Morr, F., Hotz, I., Bertram, M.H., Garth, C., Kollmann, W., Hamann, B., Hagen, H.: Moment invariants for the analysis of 2d flow fields. *IEEE Trans. Vis. Comput. Graph.* **13** (2007) 1743–1750
9. Nagaraj, S., Natarajan, V., Nanjundiah, R.S.: A gradient-based comparison measure for visual analysis of multifield data. *Comp. Graph. Forum* **30** (2011) 1101–1110
10. Albrecht, H.E.: Laser doppler and phase doppler measurement technique. second edn. Springer, New York (2003)
11. Haller, G.: Distinguished material surfaces and coherent structures in three-dimensional fluid flows. *Physica D: Nonlinear Phenomena* **149** (2001) 248 – 277
12. Anderson, J.C., Gosink, L.J., Duchaineau, M.A., Joy, K.I.: Interactive visualization of function fields by range-space segmentation. *Comp. Graph. Forum* **28** (2009) 727–734
13. Mokhtarian, F., Mackworth, A.: Scale-based description and recognition of planar curves and two-dimensional objects. *IEEE Trans. Pattern Anal. Mach. Intell.* **8** (1986) 34–43
14. Agrawal, R., Lin, K., Sawhney, H.S., Shim, K.: Fast similarity search in the presence of noise, scaling, and translation in time-series databases. In: Proc. Int. Conf. on Very Large Data Bases, San Francisco, CA, USA, Morgan Kaufmann Publishers Inc. (1995) 490–501
15. Grundy, E., Jones, M.W., Laramée, R.S., Wilson, R.P., Shepard, E.L.C.: Visualisation of Sensor Data from Animal Movement. *Comp. Graph. Forum* **28** (2009) 815–822
16. Van Wijk, J.J., Van Selow, E.R.: Cluster and calendar based visualization of time series data. In: Proc. IEEE Symposium on Information Visualization, Washington, DC, USA, IEEE Computer Society (1999) 4–9
17. Hlawatsch, M., Leube, P., Nowak, W., Weiskopf, D.: Flow radar glyphs - static visualization of unsteady flow with uncertainty. *IEEE Trans. Vis. Comput. Graph.* **17** (2011) 1949–1958
18. Yi, B., Jagadish, H.V., Faloutsos, C.: Efficient retrieval of similar time sequences under time warping. In: Proc. of the 14th Int. Conf. on Data Engineering. ICDE '98, Washington, DC, USA, IEEE Computer Society (1998) 201–208
19. Burger, R., Muigg, P., Doleisch, H., Hauser, H.: Interactive cross-detector analysis of vortical flow data. In: Coordinated and Multiple Views in Exploratory Visualization, 2007. CMV '07. Fifth Int. Conf. on. (2007) 98 –110
20. Qu, H., Chan, W., Xu, A., Chung, K., Lau, K., Guo, P.: Visual analysis of the air pollution problem in hong kong. *IEEE Trans. Vis. Comput. Graph.* **13** (2007) 1408 –1415
21. Blinn, J.F.: A generalization of algebraic surface drawing. *ACM Trans. Graph.* **1** (1982) 235–256
22. Heyer, L.J., Kruglyak, S., Yooseph, S.: Exploring expression data: identification and analysis of coexpressed genes. *Genome research* **9** (1999) 1106–1115